

Entanglement entropy in de Sitter space

Juan Maldacena* and Guilherme L. Pimentel†

* *School of Natural Sciences, Institute for Advanced Study
Princeton, NJ 08540, USA*

† *Joseph Henry Laboratories, Princeton University
Princeton, NJ 08544, USA*

We compute the entanglement entropy for some quantum field theories on de Sitter space. We consider a superhorizon size spherical surface that divides the spatial slice into two regions, with the field theory in the standard vacuum state. First, we study a free massive scalar field. Then, we consider a strongly coupled field theory with a gravity dual, computing the entanglement using the gravity solution. In even dimensions, the interesting piece of the entanglement entropy is proportional to the number of e-foldings that elapsed since the spherical region was inside the horizon. In odd dimensions it is contained in a certain finite piece. In both cases the entanglement captures the long range correlations produced by the expansion.

1. Introduction

Entanglement entropy is a useful tool to characterize states with long range quantum order in condensed matter physics (see [1,2] and references therein). It is also useful in quantum field theory to characterize the nature of the long range correlations that we have in the vacuum (see e.g. [3,4,5] and references therein).

We study the entanglement entropy for quantum field theories in de Sitter space. We choose the standard vacuum state [6,7,8] (the Euclidean, Hartle-Hawking/Bunch-Davies/Chernikov-Tagirov vacuum). We do not include dynamical gravity. In particular, the entropy we compute should not be confused with the gravitational de Sitter entropy.

Our motivation is to quantify the degree of superhorizon correlations that are generated by the cosmological expansion.

We consider a spherical surface that divides the spatial slice into the interior and exterior. We compute the entanglement entropy by tracing over the exterior. We take the size of this sphere, R , to be much bigger than the de Sitter radius, $R \gg R_{dS} = H^{-1}$, where H is Hubble's constant. Of course, for $R \ll R_{dS}$ we expect the same result as in flat space. If $R = R_{dS}$, then we would have the usual thermal density matrix in the static patch and its associated entropy¹. As usual, the entanglement entropy has a UV divergent contribution which we ignore, since it comes from local physics. For very large spheres, and in four dimensions, the finite piece has a term that goes like the area of the sphere and one that goes like the logarithm of the area. We focus on the coefficient of the logarithmic piece. In odd spacetime dimensions there are finite terms that go like positive powers of the area and a constant term. We then focus on the constant term.

We first calculate the entanglement entropy for a free massive scalar field. To determine it, one needs to find the density matrix from tracing out the degrees of freedom outside of the surface. When the spherical surface is taken all the way to the boundary of de Sitter space the problem develops an $SO(1,3)$ symmetry. This symmetry is very helpful for computing the density matrix and the associated entropy. Since we have the density matrix, it is also easy to compute the Rényi entropies.

We then study the entanglement entropy of field theories with a gravity dual. When the dual is known, we use the proposal of [10,11] to calculate the entropy. It boils down to an extremal area problem. The answer for the entanglement entropy depends drastically

¹ This can be regarded as a (UV divergent) $\mathcal{O}(G_N^0)$ correction to the gravitational entropy of de Sitter space [9].

on the properties of the gravity dual. In particular, if the gravity dual has a hyperbolic Friedman-Robertson-Walker spacetime inside, then there is a non-zero contribution at order N^2 for the “interesting” piece of the entanglement entropy. Otherwise, the order N^2 contribution vanishes.

This provides some further hints that the FRW region is indeed somehow contained in the field theory in de Sitter space [12]. More precisely, it should be contained in the superhorizon correlations of colored fields².

The paper is organized as follows. In section 2, we discuss general features of entanglement entropy in de Sitter. In section 3, we consider a free scalar field and compute its entanglement entropy. In section 4, we write holographic duals of field theories in de Sitter, and compute the entropy of spherical surfaces in these theories. We end with a discussion. Some more technical details are presented in the appendices.

2. General features of entanglement entropy in de Sitter

Entanglement entropy is defined as follows [9]. At some given time slice, we consider a closed surface Σ which separates the slice into a region inside the surface and a region outside. In a local quantum field theory we expect to have an approximate decomposition of the Hilbert space into $H = H_{in} \times H_{out}$ where H_{in} contains modes localized inside the surface and H_{out} modes localized outside. One can then define a density matrix $\rho_{in} = \text{Tr}_{H_{out}} |\psi\rangle\langle\psi|$ obtained by tracing over the outside Hilbert space. The entanglement entropy is the von Neumann entropy obtained from this density matrix:

$$S = -\text{Tr} \rho_{in} \log \rho_{in} \quad (2.1)$$

2.1. Four dimensions

We consider de Sitter space in the flat slicing

$$ds^2 = \frac{1}{(H\eta)^2} (-d\eta^2 + dx_1^2 + dx_2^2 + dx_3^2) \quad (2.2)$$

² A holographic calculation of the entanglement entropy associated to a quantum quench is presented in [13]. A quantum quench is the sudden perturbation of a pure state. The subsequent relaxation back to equilibrium can be understood in terms of the entanglement entropy of the quenched region. There, one has a contribution to the (time dependent) entropy coming from the region behind the horizon of the holographic dual.

where H is the Hubble scale and η is conformal time. We consider surfaces that sit at constant η slices. We consider a free, minimally coupled, scalar field of mass m in the usual vacuum state [6,7,8].

As in any quantum field theory, the entanglement entropy is UV divergent

$$S = S_{\text{UV-divergent}} + S_{\text{UV-finite}} \quad (2.3)$$

The UV divergencies are due to local effects and have the the form

$$S_{\text{UV-divergent}} = c_1 \frac{A}{\epsilon^2} + \log(\epsilon H)(c_2 + c_3 A m^2 + c_4 A H^2) \quad (2.4)$$

where ϵ is the UV cutoff. The first term is the well known area contribution to the entropy [3,4], coming from entanglement of particles close to the surface considered. The logarithmic terms involving c_2 and c_3 also arise in flat space. Finally, the last term involves the curvature of the bulk space³. All these UV divergent terms arise from local effects and their coefficients are the same as what we would have obtained in flat space. We have included H as a scale inside the logarithm. This is just an arbitrary definition, we could also have used m [14], when m is non-zero.

Our focus is on the UV finite terms that contain information about the long range correlations of the quantum state in de Sitter space. The entropy is invariant under the isometries of dS . This is true for both pieces in (2.3). In addition, we expect that the long distance part of the state becomes time independent. More precisely, the long range entanglement was established when these distances were subhorizon size. Once they moved outside the horizon we do not expect to be able to modify this entanglement by subsequent evolution. Thus, we expect that the long range part of the entanglement entropy should be constant as we go to late times. So, if we fix a surface in comoving x coordinates in (2.2), and we keep this surface fixed as we move to late times, $\eta \rightarrow 0$, then we naively

³ In de Sitter there is only one curvature scale, but in general we could write terms as

$$S_{\log \epsilon H} = \int_{\Sigma} \left(a R_{\mu\nu\rho\sigma} n_i^\mu n_i^\rho n_j^\nu n_j^\sigma + b R_{\mu\nu} n_i^\mu n_i^\nu + c R + d K_i^{\mu\nu} K_{i\mu\nu} + e K_{i\mu}^\mu K_{i\nu}^\nu + \dots \right) \quad (2.5)$$

where K are the extrinsic curvatures and i, j label the two normal directions and μ, ν, \dots are spacetime indices. The extrinsic curvatures also contribute to c_2 in (2.4). One could also write a term that depends on the intrinsic curvature of the surface, R_Σ , but the Gauss-Codazzi relations can be used to relate it to the other terms in (2.5).

expect that the entanglement should be constant. This expectation is not quite right because new modes are coming in at late times. However, all these modes only give rise to entanglement at short distances in comoving coordinates. The effects of this entanglement could be written in a local fashion.

In conclusion, we expect that the UV-finite piece of the entropy is given by

$$S_{\text{UV-Finite}} = c_5 A H^2 + \frac{c_6}{2} \log(A H^2) + \text{finite} = c_5 \frac{A_c}{\eta^2} + c_6 \log \eta + \text{finite} \quad (2.6)$$

where A is the proper area of the surface and A_c is the area in comoving coordinates ($A = \frac{A_c}{H^2 \eta^2}$). The finite piece is a bit ambiguous due to the presence of the logarithmic term.

The coefficient of the logarithmic term, c_6 , contains information about the long range entanglement of the state. This term looks similar to the UV divergent logarithmic term in (2.4), but they should not be confused with each other. If we had a conformal field theory in de Sitter they would be equal. However, in a non-conformal theory they are not equal ($c_6 \neq c_2$). For general surfaces, the coefficient of the logarithm will depend on two combinations of the extrinsic curvature of the surface in comoving coordinates. For simplicity we consider a sphere here⁴. This general form of the entropy, (2.6), will be confirmed by our explicit computations below.

We define the “interesting” part of the entropy to be the coefficient of the logarithm, $S_{\text{intr}} \equiv c_6$. The UV-finite area term, with coefficient c_5 , though physically interesting, is not easily calculable with our method. It receives contributions from the entanglement at distances of a few Hubble radii from the entangling surface. It would be nice to find a way to isolate this contribution and compute c_5 exactly. We could only do that in the case where the theory has a gravity dual.

2.2. Three dimensions

For three dimensional de Sitter space we can have a similar discussion.

$$\begin{aligned} S &= d_1 \frac{A}{\epsilon} + S_{\text{UV-finite}} \\ S_{\text{UV-finite}} &= d_2 A H + d_3 = d_2 \frac{A_c}{\eta} + d_3 \end{aligned} \quad (2.7)$$

⁴ It is enough to do the computation for another surface, say a cylinder, to determine the second coefficient and have a result that is valid for general surfaces [15]. In other words, for a general surface we have $c_6 = f_1 \int K_{ab} K_{ab} + f_2 \int (K_{aa})^2$ where f_1 , f_2 are some constants and K_{ab} is the extrinsic curvature of the surface within the spatial slice.

Here there is no logarithmic term. The interesting term is d_3 which is the finite piece. So we define $S_{\text{intr}} \equiv d_3$.

A similar discussion exists in all other dimensions. For even spacetime dimensions the interesting term is the logarithmic one and for odd dimensions it is the constant. One can isolate these interesting terms by taking appropriate derivatives with respect to the physical area, as done in [16] in a similar context⁵.

Note that we are considering quantum fields in a fixed spacetime. We have no gravity. And we are making no contact with the gravitational de Sitter entropy which is the area of the horizon in Planck units.

3. Entanglement entropy for a free massive scalar field in de Sitter

Here we compute the entropy of a free massive scalar field for a spherical entangling surface.

3.1. Setup of the problem

Consider, in flat coordinates, a spherical surface S^2 defined by $x_1^2 + x_2^2 + x_3^2 = R_c^2$. We consider $R_c \gg \eta$. This means that the surface is much bigger than the horizon.

If we could neglect the η dependent terms, we can take the limit $\eta \rightarrow 0$, keeping R_c fixed. This then becomes a surface on the boundary. This surface is left invariant by an $SO(1, 3)$ subgroup of the $SO(1, 4)$ de Sitter isometry group. We expect that the coefficient of the logarithmic term that we discussed above is also invariant under this group. It is therefore convenient to choose a coordinate system where $SO(1, 3)$ is realized more manifestly. This is done in two steps. First we can consider de Sitter in global coordinates, where the equal time slices are three-spheres. Then we can choose the entangling surface to be the two-sphere equator of the three-sphere. In fact, at $\eta = 0$, we can certainly map any two sphere on the boundary of de Sitter to the equator of S^3 by a de Sitter isometry. Finally, to regularize this problem we can then move back the two sphere to a very late fixed global time surface.

We can then choose a coordinate system where the $SO(1, 3)$ symmetry is realized geometrically in a simple way. Namely, this $SO(1, 3)$ is the symmetry group acting on hyperbolic slices in some coordinate system that we describe below.

⁵ See formula (1.1) of [16].

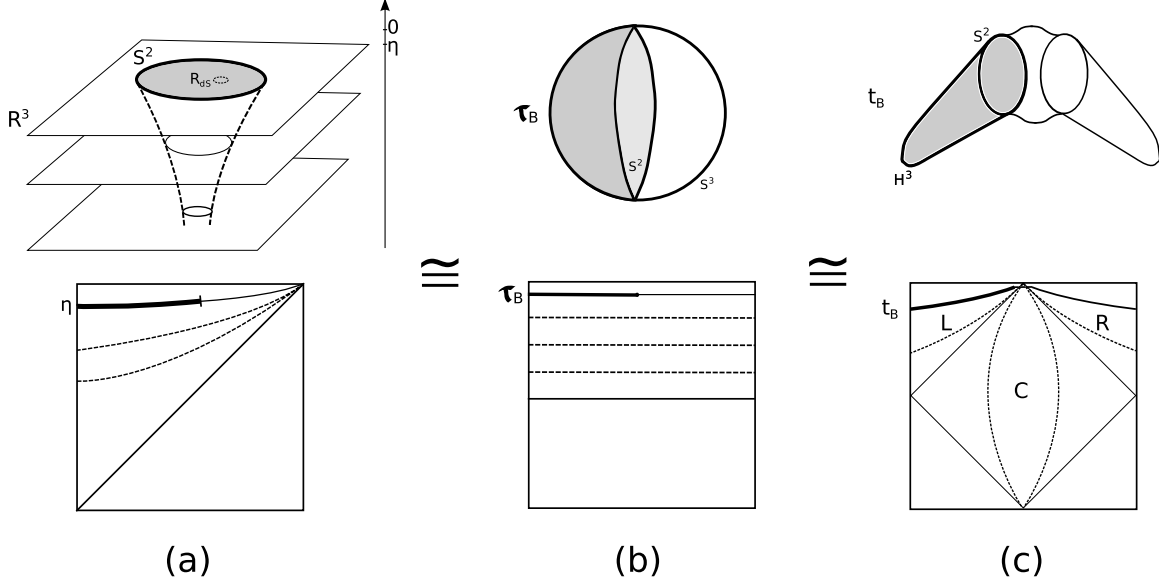


Fig. 1: Setup of the problem: (a) We consider a sphere with radius much greater than the horizon size, at late conformal time η , in flat slices. (b) This problem can be mapped to half of a 3-sphere S^3 , also with boundary S^2 , but now the equator, at late global time τ_B . (c) We can also describe this problem using hyperbolic slices. The interior of the sphere maps to the “left” (L) hyperbolic slice. The Penrose diagrams for all situations are depicted below the geometric sketches.

3.2. Wavefunctions of free fields in hyperbolic slices and the Euclidean vacuum

The hyperbolic/open slicing of de Sitter space was studied in detail in [17,18]. It can be obtained by analytic continuation of the sphere S^4 metric, sliced by S^3 s. The S^4 is described in embedding coordinates by $X_1^2 + \dots + X_5^2 = H^{-2}$. The coordinates are parametrized by angles in the following way:

$$X_5 = H^{-1} \cos \tau_E \cos \rho_E, \quad X_4 = H^{-1} \sin \tau_E, \quad X_{1,2,3} = H^{-1} \cos \tau_E \sin \rho_E n_{1,2,3} \quad (3.1)$$

where n_i are the components of a unit vector in R^3 . The metric in Euclidean signature is given by:

$$ds_E^2 = H^{-2} (d\tau_E^2 + \cos^2 \tau_E (d\rho_E^2 + \sin^2 \rho_E d\Omega_2^2)) \quad (3.2)$$

We analytically continue $X_5 \rightarrow iX_0$. Then the Lorentzian manifold is divided in three

parts, related to the Euclidean coordinates by:

$$\begin{aligned}
R : \quad & \begin{cases} \tau_E = \frac{\pi}{2} - it_R & t_R \geq 0 \\ \rho_E = -ir_R & r_R \geq 0 \end{cases} \\
C : \quad & \begin{cases} \tau_E = \tau_C & -\pi/2 \leq t_C \leq \pi/2 \\ \rho_E = \frac{\pi}{2} - ir_C & -\infty < r_C < \infty \end{cases} \\
L : \quad & \begin{cases} \tau_E = -\frac{\pi}{2} + it_L & t_L \geq 0 \\ \rho_E = -ir_L & r_L \geq 0 \end{cases}
\end{aligned} \tag{3.3}$$

The metric in each region is given by:

$$\begin{aligned}
ds_R^2 &= H^{-2}(-dt_R^2 + \sinh^2 t_R(dr_R^2 + \sinh^2 r_R d\Omega_2^2)) \\
ds_C^2 &= H^{-2}(dt_C^2 + \cos^2 t_C(-dr_C^2 + \cosh^2 r_C d\Omega_2^2)) \\
ds_L^2 &= H^{-2}(-dt_L^2 + \sinh^2 t_L(dr_L^2 + \sinh^2 r_L d\Omega_2^2))
\end{aligned} \tag{3.4}$$

We now consider a minimally coupled⁶ massive scalar field in dS_4 , with action given by $S = \frac{1}{2} \int \sqrt{-g}(-(\nabla\phi)^2 - m^2\phi^2)$. The equations of motion for the mode functions in the R or L regions are

$$\left[\frac{1}{\sinh^3 t} \frac{\partial}{\partial t} \sinh^3 t \frac{\partial}{\partial t} - \frac{1}{\sinh^2 t} \mathbf{L}_{\mathbf{H}^3}^2 + \frac{9}{4} - \nu^2 \right] u(t, r, \Omega) = 0 \tag{3.5}$$

Where $\mathbf{L}_{\mathbf{H}^3}^2$ is the Laplacian in the unit hyperboloid, and the parameter ν is

$$\nu = \sqrt{\frac{9}{4} - \frac{m^2}{H^2}} \tag{3.6}$$

When $\nu = \frac{1}{2}$ (or $\frac{m^2}{H^2} = 2$) we have a conformally coupled massless scalar. In this case we should recover the flat space answer for the entanglement entropy, since de Sitter is conformally flat. We will consider first situations where $\frac{m^2}{H^2} \geq 2$, so that $0 \leq \nu \leq 1/2$ or ν imaginary. The minimally coupled massless case corresponds to $\nu = 3/2$. We will later comment on the low mass region, $\frac{m^2}{H^2} < 2$ or $1/2 < \nu \leq 3/2$.

The wavefunctions are labeled by quantum numbers corresponding to the Casimir on H^3 and angular momentum on S^2 :

$$u_{plm} \sim \frac{H}{\sinh t} \chi_p(t) Y_{plm}(r, \Omega_2), \quad -\mathbf{L}_{\mathbf{H}^3} Y_{plm} = (1 + p^2) Y_{plm} \tag{3.7}$$

⁶ If we had a coupling to the scalar curvature $\xi R\phi^2$, we can simply shift the mass $m_{eff}^2 = m^2 + 6\xi H^2$ and consider the minimally coupled one.

The Y_{plm} are eigenfunctions on the hyperboloid, analogous to the standard spherical harmonics. Their expressions can be found in [18].

The time dependence (other than the $1/\sinh t$ factor) is contained in the functions $\chi_p(t)$. The equation of motion (3.5) is a Legendre equation and the solutions are given in terms of Legendre functions $P_a^b(x)$. In order to pick the “positive frequency” wavefunctions corresponding to the Euclidean vacuum we need to demand that they are analytic when they are continued to the lower hemisphere. These wavefunctions have support on both the Left and Right regions. This gives [18]

$$\chi_{p,\sigma} = \begin{cases} \frac{1}{2 \sinh \pi p} \left(\frac{e^{\pi p} - i\sigma e^{-i\pi\nu}}{\Gamma(\nu + ip + 1/2)} P_{\nu-1/2}^{ip}(\cosh t_R) - \frac{e^{-\pi p} - i\sigma e^{-i\pi\nu}}{\Gamma(\nu - ip + 1/2)} P_{\nu-1/2}^{-ip}(\cosh t_R) \right) \\ \frac{\sigma}{2 \sinh \pi p} \left(\frac{e^{\pi p} - i\sigma e^{-i\pi\nu}}{\Gamma(\nu + ip + 1/2)} P_{\nu-1/2}^{ip}(\cosh t_L) - \frac{e^{-\pi p} - i\sigma e^{-i\pi\nu}}{\Gamma(\nu - ip + 1/2)} P_{\nu-1/2}^{-ip}(\cosh t_L) \right) \end{cases} \quad (3.8)$$

The index σ can take the values ± 1 . For each σ the top line gives the function on the R hyperboloid and the bottom line gives the value of the function on the L hyperboloid. There are two solutions (two values of σ) because we started from two hyperboloids.

The field operator is written in terms of these mode functions as

$$\hat{\phi}(x) = \int dp \sum_{\sigma, l, m} (a_{\sigma plm} u_{\sigma plm}(x) + a_{\sigma plm}^\dagger \bar{u}_{\sigma plm}(x)) \quad (3.9)$$

To trace out the degrees of freedom in, say, the R space, we change basis to functions that have support on either the R or L regions. It does not matter which functions we choose to describe the Hilbert space. The crucial simplification of this coordinate system is that the entangling surface, when taken to the de Sitter boundary, preserves all the isometries of the H^3 slices. This implies that the entanglement is diagonal in the p, l, m indices since these are all eigenvalues of some symmetry generator. Thus, to compute this entanglement we only need to look at the analytic properties of (3.8) for each value of p .

Let us first consider the case that ν is real. For the R region we take basis functions equal to the Legendre functions $P_{\nu-1/2}^{ip}(\cosh t_R)$ and $P_{\nu-1/2}^{-ip}(\cosh t_R)$, and zero in the L region. These are the positive and negative frequency wavefunctions in the R region. We do the same in the L region. These should be properly normalized with respect to the Klein-Gordon norm, which would yield a normalization factor N_p . We can write the original mode functions, (3.8), in terms of these new ones in matricial form:

$$\begin{cases} \chi^\sigma = N_p^{-1} \sum_{q=R,L} (\alpha_q^\sigma P^q + \beta_q^\sigma \bar{P}^q) \\ \bar{\chi}^\sigma = N_p^{-1} \sum_{q=R,L} (\bar{\beta}_q^\sigma P^q + \bar{\alpha}_q^\sigma \bar{P}^q) \end{cases} \Rightarrow \chi^I = M_J^I P^J N_p^{-1} \quad (3.10)$$

$$\sigma = \pm 1, \quad P^{R,L} \equiv P_{\nu-1/2}^{ip}(\cosh t_{R,L}), \quad \chi^I \equiv \begin{pmatrix} \chi^\sigma \\ \bar{\chi}^\sigma \end{pmatrix}$$

The capital indices (I, J) run from 1 to 4, as we are grouping both the χ_σ and $\bar{\chi}_\sigma$. The coefficients α and β are simply the terms multiplying the corresponding P functions in (3.8), see appendix A for their explicit values. As the field operator should be the same under this change of basis, then it follows that:

$$\begin{aligned} \phi &= a_I \chi^I = b_J P^J N_p^{-1} \Rightarrow a_J = b_I (M^{-1})^I_J \\ M &= \begin{pmatrix} \alpha & \beta \\ \bar{\beta} & \bar{\alpha} \end{pmatrix}, \quad M^{-1} = \begin{pmatrix} \gamma & \delta \\ \bar{\delta} & \bar{\gamma} \end{pmatrix} \Rightarrow a_\sigma = \sum_{q=R,L} \gamma_{q\sigma} b_q + \bar{\delta}_{q\sigma} b_q^\dagger \end{aligned} \quad (3.11)$$

Here $a^I = (a_\sigma, a_\sigma^\dagger)$, $b^J = (b_{L,R}, b_{L,R}^\dagger)$, and $P^J = (P_{L,R}, \bar{P}_{L,R})$. M is a 2×2 matrix whose elements are 2×2 matrices. The expression for M^{-1} is the definition of δ , γ , etc. The vacuum is defined so that $a_\sigma |\Psi\rangle = 0$. We want to write $|\Psi\rangle$ in terms of the $b_{R,L}$ oscillators and the vacua associated to each of these oscillators, $b_R |R\rangle = 0$ and $b_L |L\rangle = 0$. As we are dealing with free fields, their Gaussian structure suggests the ansatz

$$|\Psi\rangle = e^{\frac{1}{2} \sum_{i,j=R,L} m_{ij} b_i^\dagger b_j^\dagger} |R\rangle |L\rangle \quad (3.12)$$

and one can solve for m_{ij} demanding that $a_\sigma |\Psi\rangle = 0$. This gives

$$m_{ij} \gamma_{j\sigma} + \bar{\delta}_{i\sigma} = 0 \Rightarrow m_{ij} = -\bar{\delta}_{i\sigma} (\gamma^{-1})_{\sigma j} \quad (3.13)$$

Using the expressions in (3.8) (see appendix A) we find for m :

$$m_{ij} = e^{i\theta} \frac{\sqrt{2} e^{-p\pi}}{\sqrt{\cosh 2\pi p + \cos 2\pi\nu}} \begin{pmatrix} \cos \pi\nu & i \sinh p\pi \\ i \sinh p\pi & \cos \pi\nu \end{pmatrix} \quad (3.14)$$

Where θ is an unimportant phase factor, which can be absorbed in the definition of the b^\dagger oscillators. In m_{ij} the normalization factors N_p drop out, so they never need to be computed.

The expression (3.12), with (3.14), needs to be simplified more before we can easily trace out the R degrees of freedom. We would like to introduce new oscillators c_L and c_R (and their adjoints) so that the original state Ψ has the form

$$|\Psi\rangle = e^{\gamma c_R^\dagger c_L^\dagger} |R\rangle' |L\rangle' \quad (3.15)$$

where $|R\rangle' |L\rangle'$ are annihilated by c_R , c_L . The details on the transformation are in appendix A. Here we state the result. The b 's and c 's are related by:

$$\begin{aligned} c_R &= u b_R + v b_R^\dagger \\ c_L &= \bar{u} b_L + \bar{v} b_L^\dagger, \quad |u|^2 - |v|^2 = 1 \end{aligned} \quad (3.16)$$

Requiring that $c_R|\Psi\rangle = \gamma c_L^\dagger|\Psi\rangle$ and $c_L|\Psi\rangle = \gamma c_R^\dagger|\Psi\rangle$ imposes constraints on u and v . The system of equations has a solution with γ given by

$$\gamma = i \frac{\sqrt{2}}{\sqrt{\cosh 2\pi p + \cos 2\pi\nu} + \sqrt{\cosh 2\pi p + \cos 2\pi\nu + 2}} \quad (3.17)$$

We have considered the case of $0 \leq \nu \leq 1/2$. For ν imaginary, (3.17) is analytic under the substitution $\nu \rightarrow i\nu$, which corresponds to substituting $\cos 2\pi\nu \rightarrow \cosh 2\pi i\nu$, so (3.17) is also valid for this range of masses. One can check directly, by redoing all the steps in the above derivation, that the same final answer is obtained if we had assumed that ν was purely imaginary.

3.3. The density matrix

The full vacuum state is the product of the vacuum state for each oscillator. Each oscillator is labelled by p, l, m . For each oscillator we can write the vacuum state as in (3.15). Expanding (3.15) and tracing over the right Hilbert space we get

$$\rho_{p,l,m} = \text{Tr}_{H_R}(|\Psi\rangle\langle\Psi|) \propto \sum_{n=0}^{\infty} |\gamma_p|^2 |n; p, l, m\rangle \langle n; p, l, m| \quad (3.18)$$

So, for given quantum numbers, the density matrix is diagonal. It takes the form $\rho_L(p) = (1 - |\gamma_p|^2) \text{diag}(1, |\gamma_p|^2, |\gamma_p|^4, \dots)$, normalized to $\text{Tr} \rho_L = 1$. The full density matrix is simply the product of the density matrix for each value of p, l, m . This reflects the fact that there is no entanglement among states with different $SO(1,3)$ quantum numbers. The density matrix for the conformally coupled case was computed before in [19].

Here, one can write the resulting density matrix as $\rho_L = e^{-\beta \mathcal{H}_{ent}}$ with \mathcal{H}_{ent} called the entanglement hamiltonian. Here it seems natural to choose $\beta = 2\pi$ as the inverse temperature of dS . Because the density matrix is diagonal, the entanglement Hamiltonian should be that of a gas of free particles, with the energy of each excitation a function of the H^3 Casimir and the mass of the scalar field. This does not appear to be related to any ordinary dynamical Hamiltonian in de Sitter. In other words, take $\rho_L \propto \text{diag}(1, |\gamma_p|^2, |\gamma_p|^4, \dots)$ then the entanglement Hamiltonian for each particles is $H_p = E_p c_p^\dagger c_p$, with $E_p = -\frac{1}{2\pi} \log |\gamma_p|^2$. For the conformally coupled scalar then $E_p = p$ and we have the entropy of a free gas in H^3 . In other words, in the conformal case the entanglement Hamiltonian coincides with the Hamiltonian of the field theory on $R \times H^3$ [20,21].

3.4. Computing the Entropy

With the density matrix (3.18) we can calculate the entropy associated to each particular set of $SO(1, 3)$ quantum numbers

$$S(p, \nu) = -\text{Tr} \rho_L(p) \log \rho_L(p) = -\log(1 - |\gamma_p|^2) - \frac{|\gamma_p|^2}{1 - |\gamma_p|^2} \log |\gamma_p|^2 \quad (3.19)$$

The final entropy is then computed by summing (3.19) over all the states. This sum translates into an integral over p and a volume integral over the hyperboloid. In other words, we use the density of states on the hyperboloid:

$$S(\nu) = V_{H^3} \int dp \mathcal{D}(p) S(p, \nu) \quad (3.20)$$

The density of states for radial functions on the hyperboloid is known for any dimensions [22]. For example, for H^3 , $\mathcal{D}(p) = \frac{p^2}{2\pi^2}$. Here V_{H^3} is the volume of the hyperboloid. This is of course infinite. This infinity is arising because we are taking the entangling surface all the way to $\eta = 0$. We can regularize the volume with a large radial cutoff in H^3 . This should roughly correspond to putting the entangling surface at a finite time. Since we are only interested in the coefficient of the logarithm, the precise way we do the cutoff at large volumes should not matter. The volume of a unit size H^3 for radius less than r_c is given by

$$V_{H^3} = V_{S^2} \int_0^{r_c} dr \sinh^2 r \sim 4\pi \left(\frac{e^{2r_c}}{8} - \frac{r_c}{2} \right) \quad (3.21)$$

The first term goes like the area of the entangling surface. The second one involves the logarithm of this area. We can also identify $r_c \rightarrow -\log \eta$. This can be understood more precisely as follows. If we fix a large t_L and we go to large r_L , then we see from (3.1)(3.3) that the corresponding surface would be at an $\eta \propto e^{-r_L}$, for large r_L . Thus, we can confidently extract the coefficient c_6 in (2.6). For such purposes we can define $V_{H^3 \text{reg}} = 2\pi$. The leading area term, proportional to e^{2r_c} depends on the details of the matching of this IR cutoff to the proper UV cutoff. These details can change its coefficient.

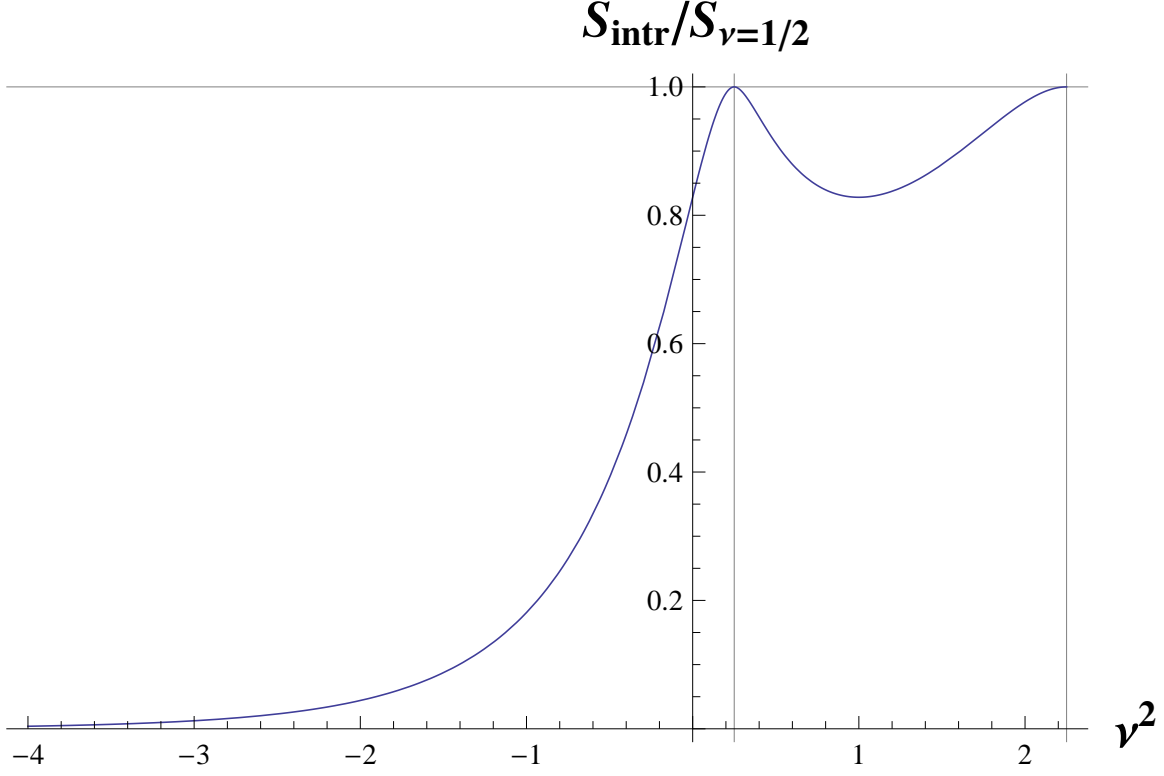


Fig. 2: Plot of the entropy $S_{intr}/S_{intr,\nu=1/2}$ of the free scalar field, normalized to the conformally coupled scalar, versus its mass parameter squared. The minimally coupled massless case corresponds to $\nu^2 = 9/4$, the conformally coupled scalar to $\nu^2 = 1/4$ and for large mass (negative ν^2) the entropy has a decaying exponential behavior.

Thus, the final answer for the logarithmic term of the entanglement entropy is

$$S = c_6 \log \eta + \text{other terms}$$

$$S_{intr} \equiv c_6 = \frac{1}{\pi} \int_0^\infty dp p^2 S(p, \nu) \quad (3.22)$$

with $S(p, \nu)$ given in (3.19), (3.17). This is plotted in fig. 2.

3.5. Extension to general dimensions

These results can be easily extended to a real massive scalar field in any number of dimensions D . Again we have hyperbolic H^{D-1} slices and the decomposition of the time dependent part of the wavefunctions is identical, provided that we replace ν by the corresponding expression in D dimensions

$$\nu^2 = \frac{(D-1)^2}{4} - \frac{m^2}{H^2} \quad (3.23)$$

Then the whole computation is identical and we get exactly the same function $S(p, \nu)$ for each mode. The final result involves integrating with the right density of states for hyperboloids in $D - 1$ dimensions which is [22]

$$\begin{aligned} \mathcal{D}_2(p) &= \frac{p}{2\pi} \tanh \pi p, \quad \mathcal{D}_3(p) = \frac{p^2}{2\pi^2} \\ \mathcal{D}_{D-1}(p) &= \frac{p^2 + \left(\frac{D-4}{2}\right)^2}{2\pi(D-3)} \mathcal{D}_{D-3}(p) = \frac{2}{(4\pi)^{\frac{D-1}{2}} \Gamma(\frac{D-1}{2})} \frac{|\Gamma(ip + \frac{D}{2} - 1)|^2}{|\Gamma(ip)|^2}, \\ -\mathbf{L}_{\mathbf{H}^{D-1}} Y_p &= \left(p^2 + \left(\frac{D-2}{2} \right)^2 \right) Y_p \end{aligned} \quad (3.24)$$

We also need to define the regularized volumes of hyperbolic space in $D - 1$ dimensions. They are related to the volume of spheres

$$V_{H^{D-1}, \text{reg}} = \begin{cases} \frac{(-1)^{\frac{D}{2}} V_{S^{D-1}}}{2} & D \text{ even} \\ \frac{(-1)^{\frac{D-1}{2}} V_{S^{D-1}}}{2} & D \text{ odd} \end{cases}, \quad V_{S^{D-1}} = \frac{2\pi^{\frac{D}{2}}}{\Gamma(\frac{D}{2})} \quad (3.25)$$

When D is even, we defined this regularized volume as minus the coefficient of $\log \eta$. When D is odd, we defined it to be the finite part after we extract the divergent terms. A derivation of these volume formulas is given in appendix B. Then the final expression for any dimension is

$$S_{\text{intr}} = V_{H^{D-1}, \text{reg}} \int_0^\infty dp \mathcal{D}_{D-1}(p) S(p, \nu) \quad (3.26)$$

with the expressions in (3.25), (3.24), (3.19), (3.17), (3.23). We have defined S_{reg} as

$$\begin{aligned} S &= S_{\text{intr}} \log \eta + \dots & \text{for } D \text{ even} \\ S &= S_{\text{intr}} + \dots & \text{for } D \text{ odd} \end{aligned} \quad (3.27)$$

where the dots denote terms that are UV divergent or that go like powers of η for small η .

3.6. Rényi Entropies

We can also use the density matrix to compute the Rényi entropies, defined as:

$$S_q = \frac{1}{1-q} \log \text{Tr} \rho^q, \quad q > 0 \quad (3.28)$$

We first calculate the Rényi entropy associated to each $SO(1, 3)$ quantum number. It is given by:

$$S_q(p, \nu) = \frac{q}{1-q} \log(1 - |\gamma_p|^2) - \frac{1}{1-q} \log(1 - |\gamma_p|^{2q}) \quad (3.29)$$

Then, just like we did for the entanglement entropy (which corresponds to $q \rightarrow 1$), one integrates (3.29) with the density of states for $D - 1$ hyperboloids:

$$S_{q,\text{intr}} = V_{H^{D-1},\text{reg}} \int_0^\infty dp \mathcal{D}_{D-1}(p) S_q(p, \nu) \quad (3.30)$$

With $S_{q,\text{intr}}$ being the finite term in the entropy, for odd dimensions, and the term that multiplies $\log \eta$, for even dimensions.

3.7. Consistency checks: conformally coupled scalar and large mass limit

As a consistency check of (3.20), we analyze the cases of the conformally coupled scalar, and of masses much bigger than the Hubble scale.

Conformally coupled scalar

For the conformally coupled scalar in any dimensions we need to set the mass parameter to $\nu = 1/2$. The entropy should be the same as that of flat space. For a spherical entangling surface, the universal term is $g_e \log \epsilon_{UV}/R$ for even dimensions, and is a finite number, g_o , for odd dimensions [20,21]. The only difference here is that we are following a surface of constant comoving area, so its radius is given by $R = R_c/(H\eta)$. So, one sees that the term that goes like $\log \eta$, in even dimensions, has the exact same origin as the UV divergent one; in particular, we expect $c_6 = g_e$ for the four dimensional case, and g_o is the finite piece in the three dimensional case.

Four dimensions:

The entropy is given by (3.22)

$$S_{\text{intr}} = \frac{1}{\pi} \int_0^\infty dp \frac{p^2}{2\pi^2} S\left(p, \frac{1}{2}\right) = \frac{1}{90} \quad (3.31)$$

This indeed coincides with the coefficient of the logarithm in the flat space result [20].

Three dimensions:

The entropy is given by:

$$\begin{aligned} S_{\text{intr}} &= V_{H^2, \text{reg}} \int \frac{d^2 p}{(2\pi)^2} \tanh \pi p S\left(p, \frac{1}{2}\right) = - \int_0^\infty p dp \tanh \pi p S\left(p, \frac{1}{2}\right) = \\ &= \frac{3\zeta(3)}{16\pi^2} - \frac{\log(2)}{8} \end{aligned} \quad (3.32)$$

This corresponds to half the value computed in [23], because there a complex scalar is considered, and also matches to half the value of the Barnes functions in [21].

Conformally coupled scalar in other dimensions

For even dimensions, S_{intr} has been reported for dimensions up to $d = 14$ in [20], and for odd dimensions, numerical values were reported up to $d = 11$ [21]. Using (3.26) we checked that the entropies agree for all the results in [20,21].

Large mass limit

Here we show the behavior of the entanglement entropy for very large mass, in three and four dimensions. The eigenvalues of the density matrix as a function of the $\text{SO}(1,3)$ Casimir are given in terms of (3.17). For large mass, there are basically two regimes, $0 < p < |\nu|$ and $p > |\nu|$

$$|\gamma_p|^2 = \begin{cases} e^{-2\pi|\nu|} & 0 < p < |\nu| \\ e^{-2\pi p} & |\nu| < p \end{cases} \quad (3.33)$$

In this regime we can approximate $|\gamma| \ll 1$ everywhere and the entropy per mode is

$$S(p) \sim -|\gamma_p|^2 \log |\gamma_p|^2 \quad (3.34)$$

Most of the contribution will come from the region $p < |\nu|$, up to $1/\nu$ corrections. This gives

$$\frac{S_{\text{intr}}}{V_{H^{D-1}, \text{reg}}} \sim \int_0^\nu dp \mathcal{D}(p) S(p) \sim (2\pi\nu e^{-2\pi\nu}) \int_0^\nu dp \mathcal{D}(p) = \begin{cases} \frac{\nu^3}{2} e^{-2\pi\nu} & d = 3 \\ \frac{\nu^4}{3\pi} e^{-2\pi\nu} & d = 4 \end{cases} \quad (3.35)$$

which is accurate up to multiplicative factors of order $(1 + \mathcal{O}(1/\nu))$.

3.8. Low mass range: $1/2 < \nu \leq 3/2$

In this low mass range the expansion of the field involves an extra mode besides the ones we discussed so far [18]. This is a mode with a special value of p . Namely $p = i(\nu - \frac{1}{2})$. This mode is necessary because all the other modes, which have real p , have wavefunctions whose leading asymptotics vanish on the S^2 equator of the S^3 future boundary. This mode has a different value for the Casimir (a different value of p) than all other modes, so it cannot be entangled with them. So we think that this mode does not contribute to the long range entanglement. It would be nice to verify this more explicitly.

Note that we can analytically continue the answer we obtained for $\nu \leq 1/2$ to larger values. We obtain an answer which has no obvious problems, so we suspect that this is the right answer for the entanglement entropy, even in this low mass range. The full result is plotted in fig. 2, and we find that for $\nu = 3/2$, which is the massless scalar, we get exactly the same result as for a conformally coupled scalar.

4. Entanglement entropy from gravity duals.

After studying free field theories in the previous section, we now consider strongly coupled field theories in de Sitter. We consider theories that have a gravity dual. Gauge gravity duality in de Sitter was studied in [24,25,26,27,28,29,30,31,32,33,34,35,36,37,38], and references there in. When a field theory has a gravity dual, it was proposed in [10] that the entanglement entropy is proportional to the area of a minimal surface that ends on the entangling surface at the AdS boundary. This formula has passed many consistency checks. It is certainly valid in simple cases such as spherical entangling surfaces [39]. Here we are considering a time dependent situation. It is then natural to use extremal surfaces but now in the full time dependent geometry [11]. This extremality condition tells us how the surface moves in the time direction as it goes into the bulk.

First, we study a CFT in de Sitter. This is a trivial case since de Sitter is conformally flat, so we can go to a conformal frame that is not time dependent and obtain the answer [10,40]. Nevertheless we will describe it in some detail because it is useful as a stepping stone for the non-conformal case. We then consider non-conformal field theories in some generality. We relegate to appendix C the discussion of a special case corresponding to a non-conformal field theory in four dimensions that comes from compactifying a five dimensional conformal field theory on a circle.

4.1. Conformal field theories in de Sitter

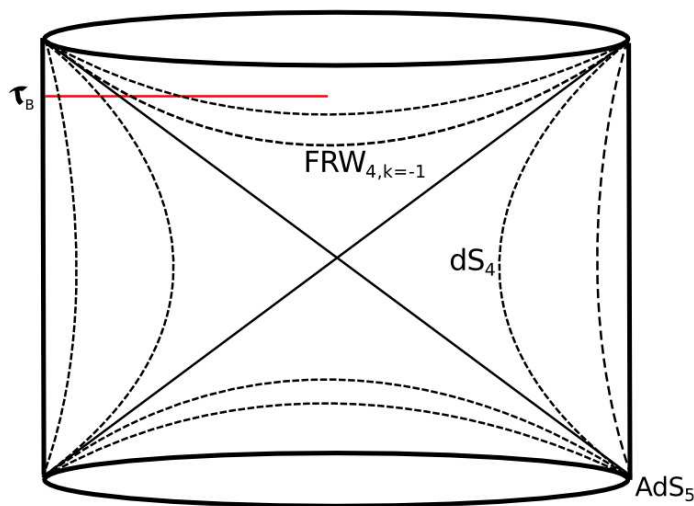


Fig. 3: The gravity dual of a CFT living on dS_4 . We slice AdS_5 with dS_4 slices. Inside the horizon we have an FRW universe with H^4 slices. The minimal surface is an H^3 that lies on a constant global time surface. The red line represents the radial direction of this H^3 , and the S^2 shrinks smoothly at the tip.

As the field theory is defined in dS_4 , it is convenient to choose a dS_4 slicing of AdS_5 . These slices cover only part of the spacetime, see fig. 3. They cover the region outside the lightcone of a point in the bulk. The interior region of this lightcone can be viewed as an FRW cosmology with hyperbolic spatial slices.

We then introduce the following coordinate systems:

1. Embedding coordinates

$$\begin{aligned} -Y_{-1}^2 - Y_0^2 + Y_1^2 + \dots + Y_4^2 &= -1 \\ ds^2 &= -dY_{-1}^2 - dY_0^2 + dY_1^2 + \dots + dY_4^2 \end{aligned} \quad (4.1)$$

2. dS_4 and FRW coordinates

2.1 dS slices

$$\begin{aligned} Y_{-1} &= \cosh \rho, \quad Y_0 = \sinh \rho \sinh \tau, \quad Y_i = \sinh \rho \cosh \tau n_i \\ ds^2 &= d\rho^2 + \sinh^2 \rho (-d\tau^2 + \cosh^2 \tau (d\alpha^2 + \cos^2 \alpha d\Omega_2)) \end{aligned} \quad (4.2)$$

2.2 FRW slices. We substitute $\rho = i\sigma$ and $\tau = -i\frac{\pi}{2} + \chi$ in (4.2).

$$\begin{aligned} Y_{-1} &= \cos \sigma, \quad Y_0 = \sin \sigma \cosh \chi, \quad Y_i = \sin \sigma \sinh \chi n_i \\ ds^2 &= -d\sigma^2 + \sin^2 \sigma (d\chi^2 + \sinh^2 \chi (d\alpha^2 + \cos^2 \alpha d\Omega_2)) \end{aligned} \quad (4.3)$$

3. Global coordinates

$$\begin{aligned} Y_{-1} &= \cosh \rho_g \cos \tau_g, \quad Y_0 = \cosh \rho_g \sin \tau_g, \quad Y_i = \sinh \rho_g n_i \\ ds^2 &= d\rho_g^2 - \cosh^2 \rho_g d\tau_g^2 + \sinh^2 \rho_g (d\alpha^2 + \cos^2 \alpha d\Omega_2) \end{aligned} \quad (4.4)$$

As the entangling surface we choose the S^2 at $\alpha = 0$, at a large time τ_B and at $\rho = \infty$. In terms of global coordinates the surface lies at a constant τ_g , or at

$$\frac{Y_0}{Y_{-1}} = \sinh \tau_B = \tan \tau_{gB}, \quad Y_4 = 0 \quad (4.5)$$

Its area is

$$A = 4\pi \int_0^{\rho_{gc}} \sinh^2 \rho_g d\rho_g \sim 4\pi \left(\frac{e^{2\rho_{gc}}}{8} - \frac{\rho_{gc}}{2} \right) \quad (4.6)$$

where ρ_{gc} is the cutoff in the global coordinates. It is convenient to express this in terms of the radial coordinate in the dS slicing using $\sinh \rho_g = \sinh \rho \cosh \tau$. In the large ρ_{gc} , ρ_c , τ_B limit we find $\rho_{gc} \approx \rho_c + \tau_B - \log 2$. Then (4.6) becomes

$$A \sim 4\pi \left(\frac{e^{2\rho_c + 2\tau_B}}{16} - \frac{1}{2}(\rho_c + \tau_B) \right) \sim 4\pi \left(\frac{1}{16(\eta \epsilon_{UV})^2} + \frac{1}{2}(\log \epsilon_{UV} + \log \eta) \right) \quad (4.7)$$

We see that the coefficients of the two logarithmic terms are the same, as is expected in any CFT. Here $\epsilon_{UV} = e^{-\rho_c}$ is the cutoff in the de Sitter frame and $\eta \sim e^{-\tau_B}$ is de Sitter conformal time.

4.2. Non-conformal theories

A simple way to get a non-conformal theory is to add a relevant perturbation to a conformal field theory. Let us first discuss the possible Euclidean geometries. Thus we consider theories on a sphere. In the interior we obtain a spherically symmetric metric and profile for the scalar field of the form

$$ds^2 = d\rho^2 + a^2(\rho)d\Omega_D^2, \quad \phi = \phi(\rho) \quad (4.8)$$

Some examples were discussed in [41,26,42]⁷. If the mass scale of the relevant perturbation is small compared to the inverse size of the sphere, the dual geometry will be a small deformation of Euclidean AdS_{D+1} . Then we find that, at the origin, $a = \rho + \mathcal{O}(\rho^3)$, and the sphere shrinks smoothly. In this case we will say that we have the “ungapped” phase. For very large ρ we expect that $\log a \propto \rho$, if we have a CFT as the UV fixed point description.

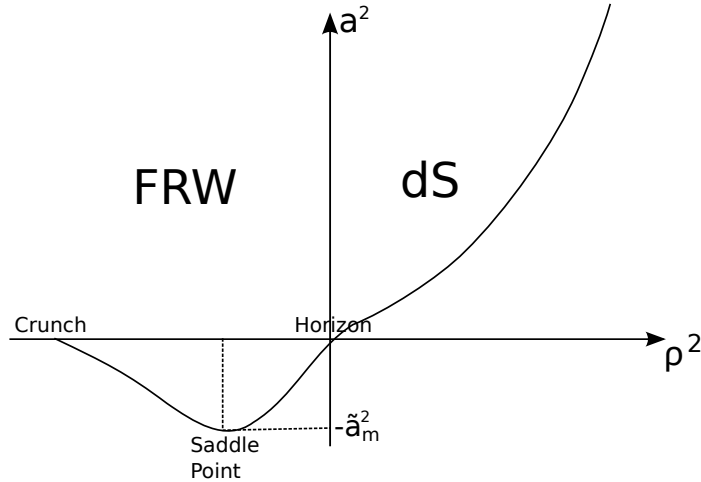


Fig. 4: The typical shape for the scale factor for the gravity dual of a CFT perturbed by a relevant operator in the “ungapped” phase. The region with negative ρ^2 corresponds to the FRW region. In that region, we see that $\tilde{a}^2 = -a^2$ reaches a maximum value, \tilde{a}_m , and then contracts again into a big crunch.

On the other hand, if the mass scale of the relevant perturbation is large compared to the inverse size of the sphere then the boundary sphere does not have to shrink when we go to the interior. For example, the space can end before we get to $a = 0$. This can happen

⁷ We are interpreting the solutions of [42] as explained in appendix A of [12]. This geometry also appears in decays of AdS space [43,42].

in multiple ways. We could have an end of the world brane at a non-zero value of a . Or some extra dimension could shrink to zero at this position. This typically happens for the holographic duals of theories with a mass gap, especially if the mass gap is much bigger than H . We call this the “gapped” phase. See [28,30,31,33,38,44,45] for some examples. In principle, the same field theory could display both phases as we vary the mass parameter of the relevant perturbation. Then, there is a large N phase transition between the two regimes⁸.

As we go to lorentzian signature, the ungapped case leads to a horizon, located at $\rho = 0$. The metric is smooth if $a = \rho + \mathcal{O}(\rho^3)$. The region behind this horizon is obtained by setting $\rho = i\sigma$ in (4.8) and $d\Omega_D^2 \rightarrow -ds_{H_D}^2$. This region looks like a Friedman-Robertson-Walker cosmology with hyperbolic spatial sections.

$$ds^2 = -d\sigma^2 + (\tilde{a}(\sigma))^2 ds_{H_D}^2, \quad \tilde{a}(\sigma) \equiv -ia(i\rho) \quad (4.9)$$

If the scalar field is non-zero at $\rho = 0$ we typically find that a singularity develops at a non-zero value of σ , with the scale factor growing from zero at $\sigma = 0$ and then decreasing again at the big crunch singularity. The scale factor then achieves a maximum somewhere in between, say at σ_m . See fig. 4.

We can choose global coordinates for dS_D

$$ds_{dS_D} = -d\tau^2 + \cosh^2 \tau (\cos^2 \alpha d\Omega_{D-2} + d\alpha^2) \quad (4.10)$$

We pick the entangling surface to be the S^{D-2} at $\alpha = 0$ and some late time τ_B . We assume that the surface stays at $\alpha = 0$ as it goes into the bulk. In that case we simply need to find how τ varies as a function of ρ as we go into the interior. We need to minimize the following action

$$S = \frac{V_{S^{D-2}}}{4G_N} \int (a \cosh \tau)^{D-2} \sqrt{d\rho^2 - a^2 d\tau^2} \quad (4.11)$$

The equations of motion simplify if we assume τ is very large and we can approximate $\cosh \tau \sim \frac{1}{2}e^\tau$. In that case the equations of motion give a first order equation for $y \equiv \frac{d\tau}{d\rho}$.

⁸ Since we are at finite volume we might not have a true phase transition. In de Sitter, thermal effects will mix the two phases. We will nevertheless restrict our attention to one of these phases at a time.

4.3. Non-conformal theories - gapped phase

In the gapped phase, we can solve the equation for y . Inserting that back into the action will give an answer that will go like $e^{(D-2)\tau_B}$ times some function which depends on the details of the solution. Thus, this produces just an area term. We can expand the action in powers of $e^{-2\tau}$ and obtain corrections to this answer. However, if the solution is such that the range of variation of τ is finite in the interior, then we do not expect that any of these corrections gives a logarithmic term (for even D) or a finite term (for odd D). Thus, in the gapped phase we get that

$$S_{\text{intr}} = 0 \quad (4.12)$$

to leading order. The discussion is similar to the one in [46,47] for a large entangling surface.

4.4. Non conformal theories - ungapped phase

In the ungapped phase, something more interesting occurs. The surface goes all the way to the horizon at $\rho = 0$. Up to that point the previous argument still applies and we expect no contributions to the interesting piece of the entropy from the region $\rho > 0$.

When the surface goes into the FRW region note that the S_{D-2} can shrink to zero at the origin of the hyperbolic slices. If we call $\rho = i\sigma$ and $\tau = \chi - i\pi/2$, then we see that the metric of the full space has the form

$$ds^2 = -d\sigma^2 + (\tilde{a}(\sigma))^2 [d\chi^2 + \sinh^2 \chi (\cos^2 \alpha d\Omega_{D-2} + d\alpha^2)] \quad (4.13)$$

where $\tilde{a}(\sigma) = -ia(i\sigma)$ is the analytic continuation of $a(\rho)$. We expect that the surface extends up to $\chi = 0$ where the S^{D-1} shrinks smoothly. Clearly this is what was happening in the conformal case discussed in the previous subsection. Thus, by continuity we expect that this also happens in this case.

More explicitly, in this region we can write the action (4.11),

$$S = \frac{V_{S^{D-2}}}{4G_N} \int (\tilde{a} \sinh \chi)^{D-2} \sqrt{-\left(\frac{d\sigma}{d\chi}\right)^2 + \tilde{a}^2} \quad (4.14)$$

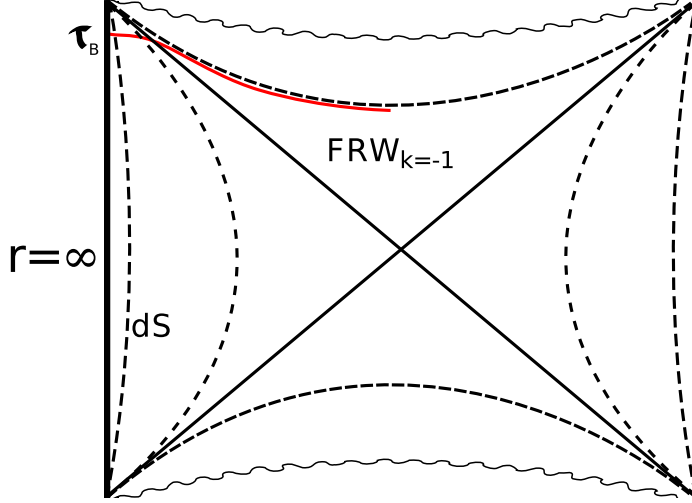


Fig. 5: The holographic setup for a non conformal field theory on de Sitter in the “ungapped” phase. We again have a region with dS_4 slices and an FRW region with hyperbolic, H_4 , slices. The extremal surface that computes the entanglement entropy goes through the horizon into the FRW region. There it approaches the slice with maximum scale factor $a = a_m$.

If we first set $\frac{d\sigma}{d\chi} = 0$, we can extremize the area by sitting at σ_m where $\tilde{a} = \tilde{a}_m$, which is the maximum value for \tilde{a} . We can then include small variations around this point. We find that we get exponentially increasing or decreasing solutions as we go away from σ_m . Since the solution needs to join into a solution with a very large value of τ_B , we expect that it will start with a value of σ at $\chi = 0$ which is exponentially close to σ_m . Then the solution stays close to σ_m up to $\chi \sim \tau_B$ and then it moves away and approaches $\sigma \sim 0$. Namely, we expect that for $\sigma \sim 0$ the solution will behave as $\chi = \tau_B - \log \sigma + \text{rest}$, where the rest has an expansion in powers of $e^{-2\tau_B}$. This then joins with the solution of the form $\tau = \tau_B - \log \rho + \text{rest}$ in the $\rho > 0$ region. The part of the solution which we denote as “rest”, has a simple expansion in powers of $e^{-2\tau_B}$, with the leading term being independent of τ_B . All those terms are not expected to contribute to the interesting part of the entanglement entropy. The qualitative form of the solution can be found in figure fig. 5.

The interesting part of the entanglement entropy comes from the region of the surface that sits near σ_m . In this region the entropy behaves as

$$S = \frac{\tilde{a}_m^{D-1}}{4G_N} V_{H^{D-1}} \quad \longrightarrow \quad S_{\text{intr}} = \frac{\tilde{a}_m^{D-1}}{4G_N} V_{H^{D-1} \text{reg}} \quad (4.15)$$

Here we got an answer which basically goes like the volume of the hyperbolic slice H^{D-1} . This should be cutoff at some value $\chi \sim \tau_B$. We have extracted the log term or the finite term, defined as the regularized volume.

Thus (4.15) gives the final expression for the entanglement entropy computed using the gravity dual. We see that the final expression is very simple. It depends only on the maximum value, \tilde{a}_m , of the scale factor in the FRW region.

Using this holographic method, and finding the precise solution for the extremal surface one can also compute the coefficient c_5 in (2.6) (or analogous terms in general dimensions). But we will not do that here.

In appendix C we discuss a particular example in more detail. The results agree with the general discussion we had here.

5. Discussion

In this paper we have computed the entanglement entropy of some quantum field theories in de Sitter space. There are interesting features that are not present in the flat space case. In flat space, a massive theory does not lead to any long range entanglement. On the other hand, in de Sitter space particle creation gives rise to a long range contribution to the entanglement. This contribution is specific to de Sitter space and does not have a flat space counterpart. We isolated this interesting part by considering a very large surface and focusing on the terms that were either logarithmic (for even dimensions) or constant (for odd dimensions) as we took the large area limit.

In the large area limit the computation can be done with relative ease thanks to a special $SO(1,D-1)$ symmetry that arises as we take the entangling surface to the boundary of dS_D . For a free field, this symmetry allowed us to separate the field modes so that the entanglement involves only two harmonic oscillator degrees of freedom at a time. So the density matrix factorizes into a product of density matrices for each pair of harmonic oscillators. The final expression for the entanglement entropy for a free field was given in (3.26). We checked that it reproduces the known answer for the case of a conformally coupled scalar. We also saw that in the large mass limit the entanglement goes as $e^{-m/H}$ which is due to the pair creation of massive particles. Since these pairs are rare, they do not produce much entanglement.

We have also studied the entanglement entropy in theories that have gravity duals. The interesting contribution to the entropy only arises when the bulk dual has a horizon. Behind the horizon there is an FRW region with hyperbolic cross sections. The scale factor of these hyperbolic cross sections grows, has a maximum, and then decreases again. The entanglement entropy comes from a surface that sits within the hyperbolic slice at the

time of maximum expansion. This gives a simple formula for the holographic entanglement entropy (4.15). From the field theory point of view, it is an N^2 term. Thus, it comes from the long range entanglement of colored fields. It is particularly interesting that the long range entanglement comes from the FRW cosmological region behind the horizon. This suggests that this FRW cosmology is indeed somehow contained in the field theory on de Sitter space [12,48]. More precisely, it is contained in colored modes that are correlated over superhorizon distances.

In the gapped phase the order N^2 contribution to the long range entanglement entropy vanishes. We expect to have an order one contribution that comes from bulk excitations which can be viewed as color singlet massive excitations in the boundary theory. From such contributions we expect an order one answer which is qualitatively similar to what we found for free massive scalar fields above.

Acknowledgements

We thank H. Liu, I. Klebanov, R. Myers, B. Safdi and A. Strominger for discussions. J.M. was supported in part by U.S. Department of Energy grant #DE-FG02-90ER40542. G.L.P. was supported by the Department of State through a Fulbright Science and Technology Fellowship and through the U.S. NSF under Grant No. PHY-0756966.

Appendix A. Bogoliubov coefficients

Here we give the explicit form of the coefficients in (3.10).

$$\begin{aligned}\alpha_R^\sigma &= \frac{e^{\pi p} - i\sigma e^{-i\pi\nu}}{\Gamma(\nu + ip + 1/2)} , & \alpha_L^\sigma &= \sigma \frac{e^{\pi p} - i\sigma e^{-i\pi\nu}}{\Gamma(\nu + ip + 1/2)} \\ \beta_R^\sigma &= -\frac{e^{-\pi p} - i\sigma e^{-i\pi\nu}}{\Gamma(\nu - ip + 1/2)} , & \beta_L^\sigma &= -\sigma \frac{e^{-\pi p} - i\sigma e^{-i\pi\nu}}{\Gamma(\nu - ip + 1/2)}\end{aligned}\tag{A.1}$$

We also find

$$\begin{aligned}\gamma_{j\sigma} &= \frac{\Gamma(\nu + ip + \frac{1}{2})ie^{\pi p + i\pi\nu}}{4 \sinh \pi p} \left(\frac{\frac{1}{ie^{\pi p + i\pi\nu} + 1}}{\frac{1}{ie^{\pi p + i\pi\nu} + 1}} - \frac{\frac{1}{ie^{\pi p + i\pi\nu} - 1}}{\frac{1}{ie^{\pi p + i\pi\nu} - 1}} \right)_{j\sigma} \\ \bar{\delta}_{j\sigma} &= \frac{\Gamma(\nu - ip + \frac{1}{2})ie^{\pi p + i\pi\nu}}{4 \sinh \pi p} \left(\frac{\frac{1}{ie^{\pi p + i\pi\nu} + e^{2\pi p}}}{\frac{1}{ie^{\pi p + i\pi\nu} + e^{2\pi p}}} - \frac{\frac{1}{ie^{\pi p + i\pi\nu} - e^{2\pi p}}}{\frac{1}{ie^{\pi p + i\pi\nu} - e^{2\pi p}}} \right)_{j\sigma}\end{aligned}\tag{A.2}$$

these were used to obtain (3.14).

We define c_R and c_L via (3.16) and the state in (3.15). We demand that $c_R|\Psi\rangle = \gamma c_L^\dagger|\Psi\rangle$, $c_L|\Psi\rangle = \gamma c_R^\dagger|\Psi\rangle$. Using (3.16) and denoting $m_{RR} = m_{LL} = \rho$, $m_{RL} = \zeta$ these two conditions become

$$\begin{aligned} (u\rho + v - \gamma v\zeta)b_R^\dagger + (u\zeta - \gamma v\rho - \gamma u)b_L^\dagger &= 0 \\ (\bar{u}\zeta - \gamma\bar{u} - \gamma\bar{v}\rho)b_R^\dagger + (\bar{u}\rho + \bar{v} - \gamma\bar{v}\zeta)b_L^\dagger &= 0 \end{aligned} \quad (\text{A.3})$$

which imply that each of the coefficients is zero.

From the structure of (A.3), one sees that under the substitution $u \rightarrow \bar{u}$, $v \rightarrow \bar{v}$ we have the same set of equations. If one tries to solve them together then $\frac{u}{v} = \frac{\bar{u}}{\bar{v}}$; hence this ratio must be real. One can show that this is indeed the case and γ is given by (3.17).

Appendix B. Regularized volume of the Hyperboloid

Here we calculate the regularized volume of a hyperboloid in $D - 1$ dimensions. We have to consider the cases of D even and D odd separately. First, note that the volume is given by the integral:

$$V_{H^{D-1}} = V_{S^{D-2}} \int_0^{\rho_c} d\rho (\sinh \rho)^{D-2} \quad (\text{B.1})$$

Now we expand the integrand:

$$\frac{V_{H^{D-1}}}{V_{S^{D-2}}} = \frac{1}{2^{D-2}} \int_0^{\rho_c} d\rho \sum_{n=0}^{D-2} \binom{D-2}{n} (-1)^n e^{(D-2-2n)\rho} \quad (\text{B.2})$$

But the integral of any exponential is given by:

$$\int_0^{\rho_c} d\rho e^{a\rho} = -\frac{1}{a} + \begin{cases} 0, & a < 0 \\ \text{divergent}, & a > 0 \end{cases} \quad (\text{B.3})$$

Now we treat even or odd dimensions separately.

Even D : Here, the integrand of (B.2) contains a term independent of ρ in the summation, which gives rise to the logarithm (a term linear in ρ_c). The term we are interested in corresponds to setting $n = D/2 - 1$:

$$V_{H^{D-1}, \text{reg}} = \frac{(-1)^{\frac{D}{2}}}{\frac{D-2}{2}} \binom{D-2}{\frac{D-2}{2}} V_{S^{D-2}} = \frac{(-1)^{\frac{D}{2}} \pi^{\frac{D-2}{2}} (D-2)!}{\frac{D-2}{2} \left(\frac{D-2}{2}\right)!^3} = \frac{(-1)^{\frac{D}{2}}}{\pi} V_{S^{D-1}} \quad (\text{B.4})$$

Odd D : Now, there is no constant term in the integrand of (B.2). Performing the summation in (B.2), and using (B.3), we get:

$$V_{H^{D-1}, \text{reg}} = -\frac{1}{2^{D-2}} \sum_{n=0}^{D-2} \binom{D-2}{n} \frac{(-1)^n}{D-2-2n} V_{S^{D-2}} = \pi^{\frac{D-2}{2}} \Gamma\left[-\frac{D-2}{2}\right] = \frac{(-1)^{\frac{D-1}{2}}}{2} V_{S^{D-1}} \quad (\text{B.5})$$

A more direct way to relate the regularized volumes of hyperbolic space to volume of the corresponding spheres is by a shift of the integration contour. We change $\rho_c \rightarrow \rho_c + i\pi$. This does not change the constant term, but we get an $i\pi$ from the log term. We then shift the contour to run from $\rho = 0$ along $\rho = i\theta$, with $0 \leq \theta \leq \pi$ and then from $i\pi$ to $i\pi + \rho_c$. The θ integral gives the volume of a sphere and the new integral with $Im(\rho) = \pi$ gives an answer which is either the same or minus the original integral. The fact that these regularized volumes are given by volume of spheres is related to the analytic continuation between AdS and dS wavefunctions [49,50].

Appendix C. Entanglement entropy for conformal field theories on $dS_4 \times S^1$

Let us first discuss the gravity dual in the Euclidean case. The boundary is $S^4 \times S^1$. This boundary also arises when we consider a thermal configuration for the field theory on S^4 . We will consider antiperiodic boundary conditions for the fermions along the S^1 . There are two solutions. One is AdS with time compactified on a circle. The other is the Schwarzschild AdS black hole. Depending on the size of the circle one or the other solution is favored [51,52]. Here we want to continue $S^4 \rightarrow dS^4$. An incomplete list of references where these geometries were explored is [28,30,31,33,38,44,45].

As a theory on dS^4 we have a scale set by the radius of the extra spatial circle. At large N we have a sharp phase transition. At finite N we can have tunneling back and forth between these phases. Here we restrict attention to one of the phases, ignoring this tunneling. The Schwarzschild AdS solution looks basically like the gapped solutions we discussed in general above. Here, the S^4 , or the dS^4 , never shrinks to zero. It can be viewed as a bubble of nothing. On the other hand, the periodically identified AdS_6 solution gives the ungapped case, with the S^4 or dS^4 shrinking, which leads to a hyperbolic FRW region behind the horizon.

Gapped phase - Cigar geometry

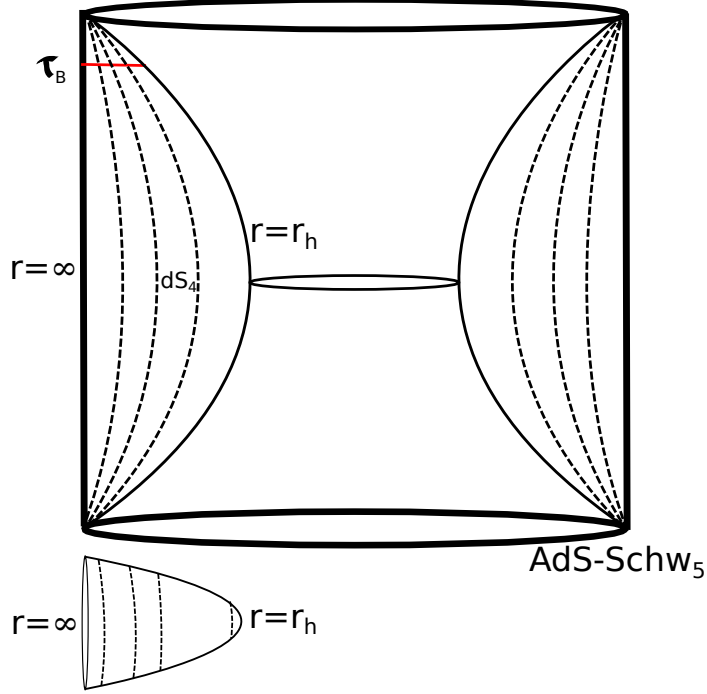


Fig. 6: The gravity dual of a 5D CFT on $dS_4 \times S^1$. The spacetime ends at $r = r_h$, where the circle shrinks in a smooth fashion. We display an extremal surface going from τ_B to the interior.

We now consider the cigar geometry. In the UV we expect to see the divergence structure to be that of a 5D CFT, but in the IR it should behave like a gapped 4D non-conformal theory. The metric is given by

$$ds^2 = f d\phi^2 + r^2 ds_{dS^4}^2 + \frac{dr^2}{f}, \quad f = 1 + r^2 - \frac{m}{r^3} \quad (C.1)$$

The period β of the ϕ circle is given in terms of r_h , the largest root of $f(r_h) = 0$, by

$$\beta = \frac{4\pi}{f'(r_h)} = \frac{4\pi r_h}{2 + 4r_h^2} \quad (C.2)$$

Note that $\beta_{max} = \pi/\sqrt{2}$. This solution only exists for $\beta \leq \beta_{max}$. This geometry is shown in fig. 6. We consider an entangling surface which is an S^2 at a large value of τ_B .

We need to consider the action

$$A \propto \int dr r^2 \cosh^2 \tau \sqrt{1 - f r^2 \tau'^2} \quad (C.3)$$

This problem was also discussed in [11]. Since we are interested in large τ_B we can approximate this by

$$A_{approx} = \int dr r^2 e^{2\tau} \sqrt{1 - f r^2 (\tau')^2} \quad (C.4)$$

If the large tau approximation is valid throughout the solution then we see that the dependence on τ_B drops out from the equation and it only appears normalizing the action. In that case the full result is proportional to the area, $e^{2\tau_B}$, with no logarithmic term. In the approximation (C.4), the equation of motion involves only τ' and τ'' . So we can define a new variable $y \equiv \tau'$ and the equation becomes first order. One can expand the equation for y and get that y has an expansion of the form $y = [-2/(3r^3) + 10/(27r^5) - 4m/(14r^6) + \dots] + a(1/r^6 + \dots)$ where a is an arbitrary coefficient representing the fact that we have one integration constant.

This undetermined coefficient should be set by requiring that the solution is smooth at $r = r_h$. If one expands the equation around $r = r_h$, assuming the solution has a power series expansion around r_h , then we get that y should have a certain fixed value at r_h and then all its powers are fixed around that point. Notice that if $y = y_h + y'_h(r - r_h) + \dots$, implies that τ is regular around that point, since $(r - r_h) \propto x^2$ where x is the proper distance from the tip.

The full solution can be written as

$$\tau = \tau_B - \int_{r_h}^{\infty} y(r) dr \quad (\text{C.5})$$

where y is independent of τ_B .

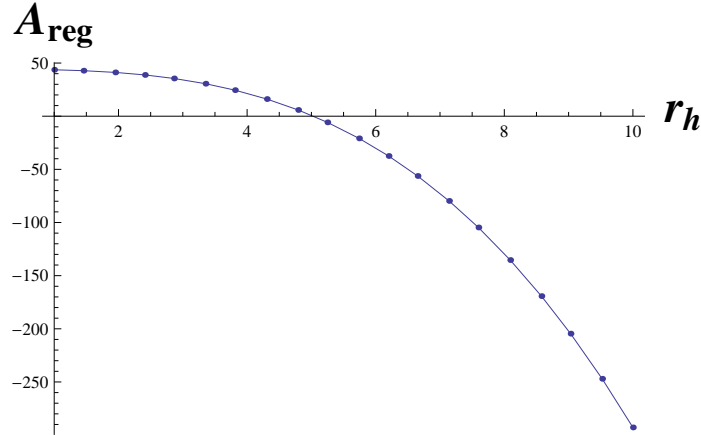


Fig. 7: The regulated area A_{reg} is defined by $A_{\text{total}} = e^{2\tau_B} A_{\text{reg}} + A_{\text{div}}$.

At large r we get $\tau - \tau_B = \frac{1}{3r^2} + \mathcal{O}(1/r^4)$ and the action (C.4) evaluates to

$$A_{\text{approx}} \propto e^{2\tau_B} \int dr \left[r^2 + \frac{4}{9} + \mathcal{O}\left(\frac{1}{r^2}\right) \right] \sim e^{2\tau_B} \left(\frac{r_c^3}{3} + \frac{4}{9}r_c + \text{finite} \right) = e^{2\tau_B} A_{\text{reg}} + A_{\text{div}} \quad (\text{C.6})$$

We see that we get the kind of UV divergencies we expect in a five dimensional theory, as expected.

These can be subtracted and we can compute the finite terms. These are plotted in fig. 7 as a function of r_h .

So far, we have computed the finite term that grows like the area. By expanding (C.3) to the next order in the $e^{-2\tau}$ expansion we can get the next term. The next term will give a constant value, independent of the area. In particular, it will not produce a logarithmic contribution. In other words, there will not be a contribution proportional to τ_B .

In conclusion, in this phase, there is no logarithmic contribution to the entanglement entropy, at order $1/G_N$ or N^2 .

Ungapped phase - Crunching geometry

Now the geometry is simply AdS_6 with an identification. This construction is described in detail in [44,45]. The resulting geometry has a big crunch singularity where the radius of the spatial circle shrinks to zero. This geometry is sometimes called “topological black hole”, as a higher dimensional generalization of the BTZ solution in 3D gravity.

It is more convenient to use a similar coordinate system as the one used to describe the cigar geometry in the previous case. The metric is given by (C.1), with $m = 0$. Those coordinates only cover the region outside of the lightcone at the origin, $r = 0$. To continue into the FRW region, one needs to use $r = i\sigma$ and $\tau = -i\pi/2 + \chi$ in (C.1).

The equation in the $r > 0$ region is such that we can make the large τ approximation and it thus reduces to a first order equation for $y = \tau' = \frac{d\tau}{dr}$. For small r , an analysis of the differential equation tells us that

$$y \sim -\frac{1}{r} - 2r^3 + \dots + b \left(r + \frac{10-7b}{2}r^3 + \dots \right) \quad (C.7)$$

where there is only one undetermined coefficient (or integration constant) which is b (it is really non-linear in b). This leads to a τ which is

$$\tau \sim -\log r - r^4 + \dots + c + b \left(r^2 + \frac{10-7b}{8}r^4 + \dots \right) \quad (C.8)$$

where c is a new integration constant. We expect that the evolution from this near horizon region to infinity only gives a constant shift. In other words, we expect that $c = \tau_B + \text{constant}$. This constant appears to depend on the value of b that is yet to be determined. We find that b should be positive in order to get a solution that goes to infinity and is non-singular.

We are now supposed to analytically continue into the *FRW* region. For that purpose we set $r = i\sigma$ and $\tau = -i\pi/2 + \chi$. Thus the equation (C.8) goes into

$$\chi \sim -\log \sigma - \sigma^4 + \dots + c + b \left(-\sigma^2 + \frac{10-7b}{8}\sigma^4 + \dots \right) \quad (\text{C.9})$$

Then we are supposed to evolve the equation. It is convenient to change variables and write the Lagrangian in terms of $\sigma(\chi)$ as:

$$A \sim \int d\chi \sigma^2 \sinh^2 \chi \sqrt{-(\sigma')^2 + \sigma^2(1 - \sigma^2)} \quad (\text{C.10})$$

In this case, at $\chi = 0$ we can set any starting point value for $\sigma(\chi = 0)$ and we have to impose that $\sigma' = 0$. Then we get only one integration constant which is $\sigma(0)$, as the second derivative is fixed by regularity of the solution to be $\sigma''(0) = -\sigma(0)(3 - 4\sigma(0)^2)$. We see that its sign depends on the starting value of $\sigma(0)$.

Since we want our critical surface to have a “large” constant value when we get to $\sigma \rightarrow 0$ as $\chi \rightarrow \infty$, we need to tune the value of $\sigma(0)$ so that it gives rise to this large constant. This can be obtained by tuning the coefficient in front of $\sigma(0)$. This critical value of $\sigma(0)$ is easy to understand. It is a solution of the equations of motion with $\sigma'(\rho) = 0$ (for a constant σ), it is a saddle point for the solution, located at $\sigma = \sqrt{3}/2$. If σ is slightly bigger than the critical value, the minimal surface will collapse into the singularity, so we tune this value to be slightly less than the critical point.

So, in conclusion, we see that the surface stays for a while at $\sigma \approx \sqrt{3}/2$ which is the critical point stated above. The value of the action (C.10) in this region is then

$$\frac{3\sqrt{3}}{16} \int_0^{\chi_c} d\chi \sinh^2 \chi = \frac{3\sqrt{3}}{16} \left[\frac{e^{2\chi_c}}{8} - \frac{\chi_c}{2} + \dots \right] \quad (\text{C.11})$$

Here $\chi_c \sim \tau_B \sim \log \eta$ is the value of χ at the transition region. Thus, we find that the interesting contribution to the entanglement entropy is coming from the FRW region.

The transition region and the solution all the way to the *AdS* boundary is expected to be universal and its action is not expected to contribute further logarithmic terms.

In conclusion, the logarithmic term gives

$$S_{\text{intr}} = \frac{R_{AdS_6}^4}{4G_N} \beta \frac{4\pi 3\sqrt{3}}{32} \quad (\text{C.12})$$

Here we repeat this computation in another coordinate system which is non-singular at the horizon. We use Kruskal-like coordinates [44,45,30]. It also makes the numerical analysis much simpler. In terms of embedding coordinates for AdS_6 :

$$\begin{aligned} -Y_{-1}^2 - Y_0^2 + Y_1^2 + \dots + Y_5^2 &= -1 \\ ds^2 &= -dY_{-1}^2 - dY_0^2 + dY_1^2 + \dots + dY_5^2 \end{aligned} \quad (C.13)$$

The Kruskal coordinates are given by:

$$\begin{aligned} Y_{-1} &= \frac{1+y^2}{1-y^2} \cosh \phi, \quad Y_5 = \frac{1+y^2}{1-y^2} \sinh \phi, \quad Y_{0,\dots,4} = \frac{2y_{0,\dots,4}}{1-y^2}, \quad y^2 \equiv -y_0^2 + y_1^2 + \dots + y_4^2 \\ ds^2 &= \frac{4}{(1-y^2)^2} (-dy_0^2 + \dots + dy_4^2) + \left(\frac{1+y^2}{1-y^2} \right)^2 d\phi^2 \end{aligned} \quad (C.14)$$

In these coordinates, the dS region corresponds to $0 < y^2 < 1$ and the FRW region to $-1 < y^2 < 0$, with the singularity located at $y^2 = -1$. The AdS boundary is at $y^2 = 1$. We can relate the pair (r, τ) and (χ, σ) , connected by the analytic continuation $(r = i\sigma, \tau = -i\pi/2 + \chi)$ to (y^2, y_0) by the formulas:

$$\begin{aligned} r &= \frac{2\sqrt{y^2}}{1-y^2}, \quad \sinh \tau = \frac{y_0}{\sqrt{y^2}} \\ \sigma &= \frac{2\sqrt{-y^2}}{1-y^2}, \quad \cosh \chi = \frac{y_0}{\sqrt{-y^2}} \end{aligned} \quad (C.15)$$

The area functional gets simplified to:

$$A = \int \sqrt{\frac{16(1+y^2)^2}{(1-y^2)^8} (y_0^2 + y^2) [(d(y^2))^2 + 4y_0 dy_0 d(y^2) - 4y^2 (dy_0)^2]} \quad (C.16)$$

If one looks for the saddle point described in the FRW coordinates, then one obtains $y^2 = -1/3$. The same situation can be described in simple fashion in terms of these coordinates. So $y^2 \sim -1/3$ for a large range of y_0 , and it crosses to the dS -sliced region at a time of order τ_B , in dS coordinates, so part of the surface just gives the volume of an H^3 , as in (C.11):

$$A \sim \frac{9}{16} \int_0^{\frac{\cosh \chi_c}{\sqrt{3}}} \sqrt{3y_0^2 - 1} dy_0 = \frac{3\sqrt{3}}{16} \left[\frac{e^{2\chi_c}}{8} - \frac{\chi_c}{2} + \dots \right] \quad (C.17)$$

Some plots for the minimal surfaces are shown in fig. 8.

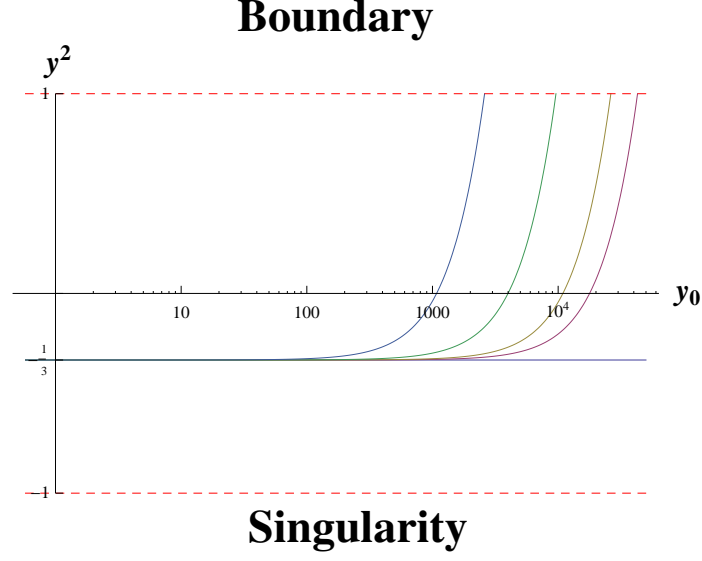


Fig. 8: We plot here the value of y^2 versus y_0 . For small y_0 the solution starts very close to the surface of maximum expansion at $y^2 = -1/3$, stays there for a while and then they go into the AdS boundary at $y^2 = 1$. The closer y_0 is to the saddle point $\tilde{y}_m^2 = -1/3$, the longer the solution will stay on this slice, giving a contribution that goes like the volume of an H^3 . Then, at a time y_0 of the order of the time the surface reaches the boundary, it exits the FRW region. The interesting (logarithmic) contribution to the entropy is coming from the volume of the H^3 surface along the FRW slice at $y^2 = -1/3$.

References

- [1] L. Amico, R. Fazio, A. Osterloh and V. Vedral, Rev. Mod. Phys. **80**, 517 (2008). [quant-ph/0703044 [QUANT-PH]].
- [2] R. Horodecki, P. Horodecki, M. Horodecki and K. Horodecki, Rev. Mod. Phys. **81**, 865 (2009). [quant-ph/0702225].
- [3] L. Bombelli, R. K. Koul, J. Lee and R. D. Sorkin, Phys. Rev. D **34**, 373 (1986)..
- [4] M. Srednicki, Phys. Rev. Lett. **71**, 666 (1993). [hep-th/9303048].
- [5] H. Casini and M. Huerta, J. Phys. A **42**, 504007 (2009). [arXiv:0905.2562 [hep-th]].
- [6] T. S. Bunch and P. C. W. Davies, Proc. Roy. Soc. Lond. A **360**, 117 (1978)..
- [7] N. A. Chernikov and E. A. Tagirov, Annales Poincare Phys. Theor. A **9**, 109 (1968)..
- [8] J. B. Hartle and S. W. Hawking, Phys. Rev. D **28**, 2960 (1983)..
- [9] C. G. Callan, Jr. and F. Wilczek, Phys. Lett. B **333**, 55 (1994). [hep-th/9401072].
- [10] S. Ryu and T. Takayanagi, Phys. Rev. Lett. **96**, 181602 (2006). [hep-th/0603001].
- [11] V. E. Hubeny, M. Rangamani and T. Takayanagi, JHEP **0707**, 062 (2007). [arXiv:0705.0016 [hep-th]].
- [12] J. Maldacena, [arXiv:1012.0274 [hep-th]].
- [13] J. Abajo-Arrestia, J. Aparicio and E. Lopez, JHEP **1011**, 149 (2010). [arXiv:1006.4090 [hep-th]].
- [14] M. P. Hertzberg and F. Wilczek, Phys. Rev. Lett. **106**, 050404 (2011). [arXiv:1007.0993 [hep-th]].
- [15] S. N. Solodukhin, Phys. Lett. B **665**, 305 (2008). [arXiv:0802.3117 [hep-th]].
- [16] H. Liu and M. Mezei, [arXiv:1202.2070 [hep-th]].
- [17] M. Bucher, A. S. Goldhaber and N. Turok, Phys. Rev. D **52**, 3314 (1995). [hep-ph/9411206].
- [18] M. Sasaki, T. Tanaka and K. Yamamoto, Phys. Rev. D **51**, 2979 (1995). [gr-qc/9412025].
- [19] G. S. Ng and A. Strominger, [arXiv:1204.1057 [hep-th]].
- [20] H. Casini and M. Huerta, Phys. Lett. B **694**, 167 (2010). [arXiv:1007.1813 [hep-th]].
- [21] J. S. Dowker, J. Phys. A **43**, 445402 (2010). [arXiv:1007.3865 [hep-th]]. J. S. Dowker, [arXiv:1009.3854 [hep-th]] and [arXiv:1012.1548 [hep-th]].
- [22] A. A. Bytsenko, G. Cognola, L. Vanzo and S. Zerbini, Phys. Rept. **266**, 1 (1996). [hep-th/9505061].
- [23] I. R. Klebanov, S. S. Pufu, S. Sachdev and B. R. Safdi, JHEP **1204**, 074 (2012). [arXiv:1111.6290 [hep-th]].
- [24] S. Hawking, J. M. Maldacena and A. Strominger, JHEP **0105**, 001 (2001) [arXiv:hep-th/0002145].
- [25] A. Buchel, P. Langfelder and J. Walcher, Annals Phys. **302**, 78 (2002) [arXiv:hep-th/0207235].

- [26] A. Buchel, Phys. Rev. D **65**, 125015 (2002). [hep-th/0203041].
- [27] A. Buchel, P. Langfelder and J. Walcher, Phys. Rev. D **67**, 024011 (2003) [arXiv:hep-th/0207214].
- [28] O. Aharony, M. Fabinger, G. T. Horowitz and E. Silverstein, JHEP **0207**, 007 (2002) [arXiv:hep-th/0204158].
- [29] V. Balasubramanian and S. F. Ross, Phys. Rev. D **66**, 086002 (2002) [arXiv:hep-th/0205290].
- [30] R. G. Cai, Phys. Lett. B **544**, 176 (2002) [arXiv:hep-th/0206223].
- [31] S. F. Ross and G. Titchener, JHEP **0502**, 021 (2005) [arXiv:hep-th/0411128].
- [32] M. Alishahiha, A. Karch, E. Silverstein and D. Tong, AIP Conf. Proc. **743**, 393 (2005) [arXiv:hep-th/0407125].
- [33] V. Balasubramanian, K. Larjo and J. Simon, Class. Quant. Grav. **22**, 4149 (2005) [arXiv:hep-th/0502111].
- [34] T. Hirayama, JHEP **0606**, 013 (2006) [arXiv:hep-th/0602258].
- [35] A. Buchel, Phys. Rev. D **74**, 046009 (2006) [arXiv:hep-th/0601013].
- [36] J. He and M. Rozali, JHEP **0709**, 089 (2007) [arXiv:hep-th/0703220].
- [37] J. A. Hutasoit, S. P. Kumar and J. Rafferty, JHEP **0904**, 063 (2009) [arXiv:0902.1658 [hep-th]].
- [38] D. Marolf, M. Rangamani and M. Van Raamsdonk, arXiv:1007.3996 [hep-th].
- [39] H. Casini, M. Huerta and R. C. Myers, JHEP **1105**, 036 (2011). [arXiv:1102.0440 [hep-th]].
- [40] M. Li and Y. Pang, JHEP **1107**, 053 (2011). [arXiv:1105.0038 [hep-th]].
- [41] A. Buchel and A. A. Tseytlin, Phys. Rev. D **65**, 085019 (2002). [hep-th/0111017].
- [42] T. Hertog and G. T. Horowitz, JHEP **0407**, 073 (2004). [hep-th/0406134]. T. Hertog and G. T. Horowitz, JHEP **0504**, 005 (2005). [hep-th/0503071].
- [43] S. R. Coleman and F. De Luccia, Phys. Rev. D **21**, 3305 (1980)..
- [44] M. Banados, Phys. Rev. D **57**, 1068 (1998). [gr-qc/9703040].
- [45] M. Banados, A. Gomberoff and C. Martinez, Class. Quant. Grav. **15**, 3575 (1998). [hep-th/9805087].
- [46] I. R. Klebanov, D. Kutasov and A. Murugan, Nucl. Phys. B **796**, 274 (2008). [arXiv:0709.2140 [hep-th]].
- [47] I. R. Klebanov, T. Nishioka, S. S. Pufu and B. R. Safdi, JHEP **1207**, 001 (2012). [arXiv:1204.4160 [hep-th]].
- [48] J. L. F. Barbon and E. Rabinovici, JHEP **1104**, 044 (2011). [arXiv:1102.3015 [hep-th]].
- [49] J. M. Maldacena, JHEP **0305**, 013 (2003). [astro-ph/0210603].
- [50] D. Harlow and D. Stanford, [arXiv:1104.2621 [hep-th]].
- [51] S. W. Hawking and D. N. Page, Commun. Math. Phys. **87**, 577 (1983)..
- [52] E. Witten, Adv. Theor. Math. Phys. **2**, 505 (1998). [hep-th/9803131].